Non-adiabatic effects in the $\tilde{A}\,^2B_2$ and $\tilde{B}^2A_1$ states of $CH_2F_2^+$ through coupling vibrational modes

Journal of Physics: Conference Series **759** (2016) 012058 doi:10.1088/1742-6596/759/1/012058

Non-adiabatic effects in the $\tilde{A}^2B_2$ and $\tilde{B}^2A_1$ states of $CH_2F_2^+$ through coupling vibrational modes

Rudraditya Sarkar

School of Chemistry, University of Hyderabad, Hyderabad-500046, India

E-mail: rudra.smgr@gmail.com

Abstract. Vibronic coupling between the two energetically close-lying excited electronic states ($\widetilde{A}^2B_2$ and $\widetilde{B}^2A_1$) of $CH_2F_2^+$ is studied in this article. A reduced dimensional model Hamiltonian is constructed in a diabatic representation and using standard vibronic coupling theory. A detailed topographical analysis of the $\widetilde{A}$-$\widetilde{B}$ coupled surfaces is presented here and nuclear dynamics study on these surfaces is also studied by using time-dependent wavepacket propagation approach.

1. Introduction

The photophysics of difluoromethane (Freon 32) received renewed attention of experimentalists [1, 2, 3, 4] over the last few decades due its applicability in refrigerant industry instead of chlorofluorocarbons. Only a few theoretical calculations of its cationic electronic states [5] are available in the literature. Recently we focussed on the vibronic dynamics of the cationic electronic states of difluoromethane [6] by using the multi-states-multi-modes (MSMM) vibronic coupling theory developed by Köppel, Domcke and Cederbaum [7]. In this article, we mainly concentrate on the vibronic interaction between the two energetically close-lying $\widetilde{A}^2B_2$ and $\widetilde{B}^2A_1$ excited electronic states of cationic difluoromethane ($CH_2F_2^+$). A detailed account of the effect of individual coupling vibrational modes as well as the cumulative effect of all coupling vibrational modes on the coupled $\widetilde{A}-\widetilde{B}$ states is discussed here. The internal conversion dynamics of the excited $\widetilde{B}^2A_1$ electronic state to the energetically lower $\widetilde{A}^2B_2$ electronic state of $CH_2F_2^+$ is discussed.

2. Theoretical methodology: The vibronic coupling model

The first ($\widetilde{A}^2B_2$) and second ($\widetilde{B}^2A_1$) excited states of difluoromethane radical cation originate from removal of one electron from the occupied b_2 and a_1 molecular orbitals (MOs), respectively, at its ground electronic state of neutral difluoromethane belonging to C_{2v} equilibrium symmetry. The selection of these two states are made because of their energetic proximity. As we are dealing with two electronic states of $CH_2F_2^+$, the constructed model diabatic vibronic Hamiltonian is represented by a $2\otimes2$ matrix,

$$\mathcal{H} = -\frac{1}{2}\sum_{i\in a_1,a_2,b_1,b_2}\omega_i\left(\frac{\partial^2}{\partial Q_i^2}\right)\mathbf{1} + \begin{pmatrix}\mathcal{H}_{11} & \mathcal{H}_{12}\\ \mathcal{H}_{21} & \mathcal{H}_{22}\end{pmatrix}. \quad (1)$$

Where first term of Eq. 1 represents the kinetic energy of the reference state and **1** represents a (2 × 2) unit matrix. The diagonal matrix element of the second term of Eq. 1, (H_{11}/H_{22}), represents the diabatic electronic energy of the cationic electronic states and the off-diagonal element of the second term of Eq. 1, (H_{12}/H_{21}), represents the coupling between them. All the elements (H_{ij}) of this matrix are function of the dimensionless normal coordinate (NC) of the vibrational modes of neutral reference. The dimensionless NCs are represented here, as Q_g and Q_u, for totally symmetric vibrational modes and coupling vibrational modes, respectively. The nine vibrational modes of CH_2F_2 transform according to the following IREPs of C_{2v} symmetry point group

$$\Gamma = 4a_1 + 1a_2 + 2b_1 + 2b_2. \tag{2}$$

Elementary symmetry selection rule is presented in Eq. 3, allows coupling of $\widetilde{A}$ and $\widetilde{B}$ states (in first order) through the vibrational modes of b_2 symmetry

$$B_2 \otimes b_2 \otimes A_1 \supset A_1. \tag{3}$$

Where the symmetry of electronic states and vibrational modes are denoted by the upper and lower case letters, respectively. The matrix elements of the vibronic Hamiltonian (cf. Eq. 1) are expanded in a Taylor series as

$$H_{ii} = \sum_{k\in a_1} \frac{1}{2}\omega_k {Q_g^k}^2 + \sum_{k\in b_2} \frac{1}{2}\omega_k {Q_u^k}^2 + E_i + \sum_{k\in a_1} \kappa_k^i Q_g^k + \sum_{k\in a_1} \frac{1}{2}\gamma_k^i {Q_g^k}^2 + \sum_{k\in b_1,b_2,a_2} \frac{1}{2}\gamma_k^i {Q_u^k}^2 \tag{4}$$

$$H_{ij} = \sum_{k\in b_2} \lambda_k^{i-j} Q_u^k. \tag{5}$$

The first two terms in Eq. 4 describe the harmonic potential energy of neutral molecule in its electronic ground state and corresponding ω_k values are the harmonic frequencies of the vibrational modes. The term E_i represents the vertical ionization energies of the $\widetilde{A}$ and $\widetilde{B}$ electronic states. The term κ_k corresponds to the linear intra-state coupling parameter of the totally symmetric (a_1) vibrational modes, whereas the term γ_k represents the quadratic intra-state coupling parameters for all vibrational modes. The off-diagonal coupling term, λ_k^{i-j} corresponds to the linear inter-state coupling parameter between $\widetilde{A}$ and $\widetilde{B}$ through coupling vibrational modes.

The adiabatic potential energy along a coupling vibrational mode is given by

$$V_{1,2}(Q_u^k) = \frac{1}{2}\omega_k {Q_u^k}^2 + \frac{1}{2}(\gamma_k^2 + \gamma_k^1){Q_u^k}^2 + \frac{1}{2}(E_1 + E_2) \mp \sqrt{\left\{(E_1 - E_2) + \frac{1}{2}(\gamma_k^2 - \gamma_k^1)\right\}^2 + 4\lambda^2 {Q_u^k}^2} \tag{6}$$

A characteristic feature of new minima is observed in lower adiabatic surface $V_1(Q_u^k)$, whereas the upper surface becomes steeper. The symmetry of the nuclear geometry at the new minima is lower than the symmetry of equilibrium geometry of the reference state, this phenomenon is known as ″the breaking of molecular symmetry″. It is known that the symmetry breaking is simply a consequence of repulsion of the diabatic surfaces via the vibronic coupling [7]. The value of dimensionless normal coordinate at the minimum of the lower adiabatic PES is represented by following equation (excluding the γ_k^i):

$$Q_u^k \left(\omega_k - \frac{\lambda^2}{\sqrt{\left(\frac{E_2 - E_1}{2}\right)^2 + \lambda^2 {Q_u^k}^2}}\right) = 0. \tag{7}$$

In this equation, $\Delta=\frac{E_2-E_1}{2}$ and $x=\frac{\lambda^2}{\omega_k\Delta}$ and x is a dimensionless quantity. The three roots of Eq. 6 have the following forms:

$$Q_u^k = 0; \quad Q_u^k = \pm\frac{\lambda}{\omega_k}\sqrt{1-\frac{1}{x^2}}. \tag{8}$$

If the value of $x < 1$, then the second and third roots of Eq. 7 become imaginary. So the validity of second and third roots remain only when $x \geq 1$ and when $x < 1$ first root $Q_u^k = 0$ is valid. As a result, two equivalent minima form at $Q_u^k \neq 0$ in the lower adiabatic PES when $x > 1$ and the previous minimum at $Q_u^k = 0$ is converted as local maximum. The stabilization energy due to this symmetry breaking phenomenon is $E_s = \Delta\left(\frac{(1-x)^2}{2x}\right)$. No symmetry breaking occur for $x < 1$ and molecule does not get any stabilization due to this phenomenon. Only just above the threshold value of $x = 1$, the stabilization energy quadratically increases with x, whereas at the larger value of x, a linear dependency is observed.

After inclusion of M number of coupling vibrational modes in Eq. 6, the generalized formula of x becomes:

$$x = \sum_{k=1}^{M} x_k. \tag{9}$$

Where, x_k is the dimensionless x parameter for k^{th} coupling mode and $x_k = \frac{\lambda_k^2}{\omega_k\Delta}$. It is seen from Eq. 9 that due to multi-mode effect x is generated from the contribution (x_k) of each coupling vibrational mode. In this way symmetry breaking phenomenon of a molecule becomes cumulative effect of all coupling vibrational modes. So in order to give an explanation of Eq. 9, one can say that if a single coupling vibrational mode fails to introduce a minimum at $V_1(Q_u^k)$ at $Q_u^k \neq 0$, then due to the multi-mode effect of the other coupling vibrational modes, there will be a possibility to form a minimum in the Q_u^k sub-space under the condition of $x \geq 1$.

3. Results and discussion

In the recent past we established a diabatic vibronic coupling model for the first four electronic states of $CH_2F_2^+$ by performing extensive electronic structure calculations and reported the vibronic energy level structure of these electronic states [6]. In this article we consider the first ($\widetilde{A}^2B_2$) and second ($\widetilde{B}^2A_1$) excited electronic states of $CH_2F_2^+$ because of their energetic proximity ($\sim$0.40 eV). It is found that the vibronic structures of three excited states, $\widetilde{A}^2B_2$, $\widetilde{B}^2A_1$ and $\widetilde{C}^2A_2$ of $CH_2F_2^+$ are highly overlapping and they form the second photoelectron band of CH_2F_2 [2, 6]. These three states are coupled through multiple conical intersections (CIs) and are well separated from the ground electronic states ($\widetilde{X}^2B_1$) of $CH_2F_2^+$ [6].

The two vibrational modes of b_2 symmetry are represented as ν_8 and ν_9 vibrational modes in our previous paper [6]. The same representation is followed in this article. The vibrational frequencies, first-order (κ) and second-order (γ) intra-state coupling parameters of totally-symmetric modes (represented as ν_1,ν_2, ν_3 and ν_4) and the γ value of ν_8 and ν_9 vibrational modes are reproduced here and given in Table 1. The vertical ionization energies of considered states and the inter-state coupling (λ) of ν_8 and ν_9 vibrational modes are listed in Table 2. It is noted that all the coupling parameters and VIEs are calculated by CAS(14,11)SCF-MRCI level of theory with cc-pVTZ basis set. The effect of inter-state coupling through these vibrational modes ν_8 and ν_9 are presented in Figs. 1 and 2, respectively.

The individual dimensionless x_k parameter values for the coupling modes ν_8 and ν_9 are calculated by using the parameters from Tables 1 and 2 and those values are given in Table 2. It is clear from this table that both the values are lower than the threshold value of x_k =1 (cf. Sec. 2). Thus both these coupling vibrational modes unable to create double minima at the lower adiabatic surface $[V_1(Q_u^k)]$ due to their individual effect on the coupled-surfaces. The individual

Table 1. The vibrational frequencies, κ and γ values of totally symmetric (a_1) and b_2 symmetric vibrational modes are reproduced here from Ref. [6]. The κ and γ values of $\widetilde{A}^2B_2$ and $\widetilde{B}^2A_1$ (in parentheses) of $CH_2F_2^+$ are listed here.

Vibrational mode	Frequencies (eV)	κ (eV)	γ (eV)
$\nu_1(a_1)$	0.3867	0.0582 (-0.1078)	0.0061 (-0.0105)
$\nu_2(a_1)$	0.1948	0.1614 (0.2303)	0.0131 (0.0033)
$\nu_3(a_1)$	0.1421	-0.2717 (-0.0459)	0.0070 (-0.0236)
$\nu_4(a_1)$	0.0667	0.1635 (-0.1275)	-0.0263 (0.0014)
$\nu_8(b_2)$	0.1852		-0.0467 (-0.0068)
$\nu_9(b_2)$	0.1414		-0.1005 (0.0097)

vibronic coupling effect of these two coupling vibrational modes is reflected in the curvature of two PESs (cf. Figs. 1 and 2): one without considering the inter-state vibronic coupling (λ) and another with the inclusion of λ. The upper coupled-surface V_2, is steeper near the minimum at Q_u^k =0 than the upper uncoupled-surface, whereas the lower coupled-surface V_1 is relatively flat compared to the lower uncoupled-surface. This scenario is depicted in both Figs. 1 and 2, for the individual effect of ν_8 and ν_9 coupling vibrational modes, respectively. In these figures dashed lines reprsent the coupled-surfaces and the solid line represent the uncoupled surfaces. So it is established that the symmetry breaking and the formation of double minima at the coupled lower adiabatic surface is not possible due to the two-states-single-mode interaction. We mentioned in the Sec. 2. that the lowering of symmetry of the coupled lower surface also occurs due to the cumulative interaction of all participating coupling vibrational (here, ν_8 and ν_9) modes. The cumulative dimesionless x parameter value ($\sim$1.042) of these two coupling vibrational modes is just above the threshold value of x =1, which suggests a lowering of symmetry of the lower coupled surface due to the simultaneous distortion along two coupling vibrational modes. As a result of this two-states-multi-modes interaction, the lower coupled surface gets stabilization in (Q_u^8, Q_u^9) sub-space and the upper coupled surface becomes steeper.

Table 2. The vertical ionization energies of the $\widetilde{A}^2B_2$ and $\widetilde{B}^2A_1$ electronic states of $CH_2F_2^+$ and the inter-state coupling parameters between these two states are reproduced here from Ref. [6]. The dimensionless x_k parameters and excitation strength are tabulated in last two columns in the table, respectively.

Electronic state	Vertical ionization energy (eV)	Vibrational mode	Inter-state coupling parameter (λ (eV))	Dimensionless x_k parameter	Excitation strength
$\widetilde{A}^2B_2$	15.34	ν_8	0.0983	0.2609	0.14
$\widetilde{B}^2A_1$	15.74	ν_9	0.1487	0.7810	0.55

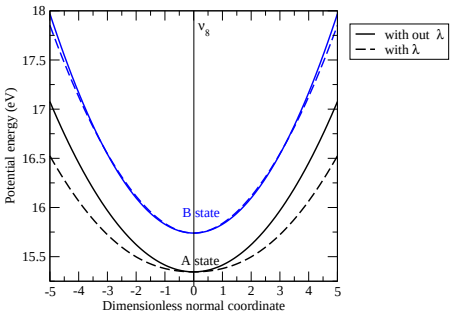

Figure 1. The effect of inter-state coupling between the $\widetilde{A}^2B_2$ and $\widetilde{B}^2A_1$ electronic states of $CH_2F_2^+$ through ν_8 vibrational mode is shown here. The solid (black and blue) lines represent the 1-D PESs in absence of inter-state coupling and the dashed (black and blue) lines represent the 1-D PESs in presence of inter-state coupling between these two states.

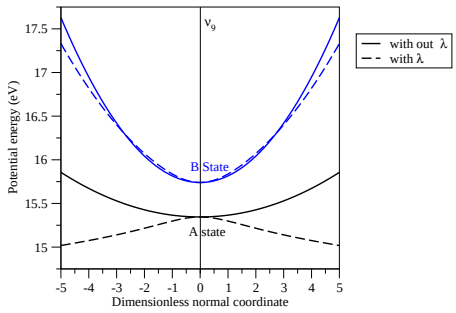

Figure 2. The effect of inter-state coupling between the $\widetilde{A}^2B_2$ and $\widetilde{B}^2A_1$ electronic states of $CH_2F_2^+$ through ν_9 vibrational mode is shown here. The solid (black and blue) lines represent the 1-D PESs in absence of inter-state coupling and the dashed (black and blue) lines represent the 1-D PESs in presence of inter-state coupling between these two states.

The internal conversion (IC) dynamics between the doublet $\widetilde{A}$ and $\widetilde{B}$ states of $CH_2F_2^+$ via $\widetilde{A}$-$\widetilde{B}$ conical intersections is studied by time-dependent wavepacket propagation approach as implemented in MCTDH programing modules [8, 9, 10, 11, 12]. The decay and growth of adiabatic (solid line) and diabatic (dashed line) electronic populations are measured by keeping the initial wavepacket in the $\widetilde{B}$ state of $CH_2F_2^+$ and is plotted in Fig. 3. The value of electronic population of $\widetilde{B}$ state is 1.0 (diabatic) and 0.67 (adiabatic) at t=0 fs and it rapidly decays to the $\widetilde{A}$ state of $CH_2F_2^+$. The indication of the latter phenomena is accounted by the electronic population growth of the latter state. From Fig. 3, it can be seen that the rate of IC via adiabatic path is faster than the diabatic path. The rate of electronic population transfer from $\widetilde{B}$ state to $\widetilde{A}$ state is found to be ∼5 fs and ∼14 fs, in adiabatic and diabatic framework, respectively. Since, the coupling strength (excitation strength) of ν_9 vibrational mode is ∼4 times higher than the vibrational mode ν_8 (cf. Table 2), the contribution of ν_9 vibrational mode is higher in this electronic population transfer. The quasi-degeneracy between the $\widetilde{A}$-$\widetilde{B}$ CIs and the energy minimum of $\widetilde{B}$ state, is another factor for this rapid IC from the $\widetilde{B}$ state to $\widetilde{A}$ state of $CH_2F_2^+$. The calculated energy of the minimum of $\widetilde{A}$-$\widetilde{B}$ CIs is 15.47 eV [13] (within second-order approximation) and the energy minimum of $\widetilde{B}$ state is 15.46 eV [13]. The location of energy minimum of $\widetilde{B}$ state is only ∼0.01 eV lower than the $\widetilde{A}$-$\widetilde{B}$ CIs, which allows a strong mixing of the lower vibrational levels of $\widetilde{B}$ state with the higher vibrational levels of $\widetilde{A}$ state. This causes a huge broadening of the spectral profile of these states. The effect of coupling vibrational modes on the $\widetilde{A}$-$\widetilde{B}$ coupled state spectral broadening is shown in Fig. 4. The effect of ν_8 and ν_9 coupling vibrational modes along with the totally symmetric vibrational modes are shown in panels a and b, respectively in the same figure. From the Fig. 4, it can be seen that the spectral broadening of panel b is higher than the panel a, which is in good accord with the higher coupling strength of ν_9 vibrational mode.

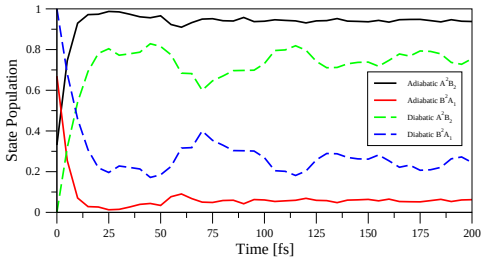

Figure 3. Adiabatic and diabatic state population analysis of the $\widetilde{B}^2A_1$ state as a function of time in femto-second, keeping the initial wavepacket in $\widetilde{B}$ state in the coupled $\widetilde{A}-\widetilde{B}$ surface of $CH_2F_2^+$.

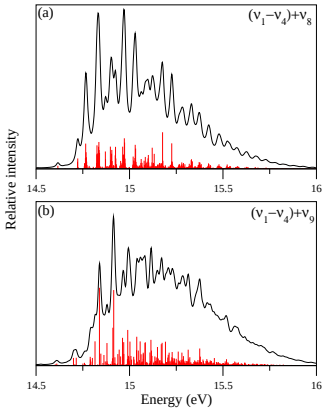

Figure 4. The effect of ν_8 and ν_9 coupling vibrational modes along with totally symmetric vibrational modes on the coupled $\widetilde{A}$-$\widetilde{B}$ state spectrum are shown in panel a and b, respectively.

4. Summary

A theoretical account of vibronic coupling between the two closely lying excited states ($\widetilde{A}^2B_2$ and $\widetilde{B}^2A_1$) of $CH_2F_2^+$ is presented in this article. A model $2\otimes2$ vibronic Hamiltonian is constructed for the purpose. The effect of coupling vibrational modes (ν_8 and ν_9) on the coupled $\widetilde{A}^2B_2$-$\widetilde{B}^2A_1$ surface is studied here by constructing the two-states-single-mode as well as two-states-multi-modes model Hamiltonian. The result shows that the symmetry breaking and stabilization of lower coupled adiabatic surface is not possible through single mode interaction rather it is possible via cummulative interaction of both coupling modes. The presence of moderate inter-state coupling and the quasi-degeneracy between the $\widetilde{A}-\widetilde{B}$ CIs with the minimum of $\widetilde{B}$ state facilitates the internal conversion between these two states.

Acknowledgements

Rudraditya Sarkar acknowledges UGC, New Delhi, India for his doctoral fellowship. Prof. Susanta Mahapatra, University of Hyderabad, is highly acknowledged for his guidance to shape up this article and valuable discussions.

References

[1] C. R. Brundle, M. B. Robin and H. Basch 1970 J. Chem. Phys. **53**, 2196.
[2] T. Pradeep and D. A. Shirley 1993 J. Electron Spectrosc. Relat. Phenom. **66**, 125.
[3] D. P. Seccombe, R. P. Tuckett and B. O. Fisher 2001 J. Chem. Phys. **114**, 4074.
[4] P. W. Forysinski, P. Zielke, D. Luckhaus, and R. Signorell 2010 Phys. Chem. Chem. Phys. **12**, 3121.
[5] K. Takeshita 1990 Chem. Phys. Lett. **165**, 232.
[6] R. Sarkar and S. Mahapatra 2015 Molecular Physics. **113**, 3073.
[7] H. Köppel, W. Domcke, and L. S. Cederbaum 1984 Adv. Chem. Phys. **57**, 59.
[8] L. S. Cederbaum, W. Domcke, H. Köppel, and W. von Niessen 1977 Chem. Phys. **26**, 169.
[9] H.-D. Meyer, U. Manthe and L.S. Cederbaum 1990 Chem. Phys. Lett. **165**, 73.
[10] U. Manthe, H.-D. Meyer and L.S. Cederbaum 1992 J. Chem. Phys. **97**, 3199.
[11] M.H. Beck, A. Jäckle, G.A. Worth, H.-D. Meyer 2000 Phys. Rep. **324**, 1.
[12] G. A. Worth, M. H. Beck, A. Jäckle, and H.-D. Meyer The mctdh package, Version 8.4, (2007), University of Heidelberg, Heidelberg, Germany. See: http://mctdh.uni-hd.de.
[13] R. Sarkar and S. Mahapatra 2016 J. Phys. Chem. A. 120, 3504.